2021

Gas exchange measurements in the unsteady state

Aaron J. Saathoff

Jonathan Mark Welles

Received: 30 October 2020 | Accepted: 19 August 2021

DOI: 10.1111/pce.14178

ORIGINAL ARTICLE

Plant, Cell & Environment WILEY

Gas exchange measurements in the unsteady state

Aaron J. Saathoff[1,2] | Jon Welles[1]

[1]LI-COR Biosciences, Lincoln, Nebraska, USA

[2]School of Natural Resources, University of Nebraska, Lincoln, Nebraska, USA

Correspondence
Aaron J. Saathoff, LI-COR Biosciences, 4647 Superior Street, Lincoln, NE 68504, USA.
Email: ajsaathoff1@gmail.com

Abstract

Leaf level gas exchange is a widely used technique that provides real-time measurement of leaf physiological properties, including CO_2 assimilation (A), stomatal conductance to water vapour (g_{sw}) and intercellular CO_2 (C_i). Modern open-path gas exchange systems offer greater portability than the laboratory-built systems of the past and take advantage of high-precision infrared gas analyzers and optimized system design. However, the basic measurement paradigm has long required steady-state conditions for accurate measurement. For CO_2 response curves, this requirement has meant that each point on the curve needs 1–3 min and a full response curve generally requires 20–35 min to obtain a sufficient number of points to estimate parameters such as the maximum velocity of carboxylation ($V_{c,max}$) and the maximum rate of electron transport (J_{max}). For survey measurements, the steady-state requirement has meant that accurate measurement of assimilation has required about 1–2 min. However, steady-state conditions are not a strict prerequisite for accurate gas exchange measurements. Here, we present a new method, termed dynamic assimilation, that is based on first principles and allows for more rapid gas exchange measurements, helping to make the technique more useful for high throughput applications.

KEYWORDS
dynamic assimilation, gas exchange, photosynthesis, RACiR, rapid A/Ci, steady-state, survey measurement

1 | INTRODUCTION

The need to provide more fuel, fiber and food for a growing global population in the face of resource constraints as well as the challenge of climate change provides much of the impetus for current photosynthesis research (Ehrlich & Harte, 2015; Jaggard, Qi, & Ober, 2010; Ray, Mueller, West, & Foley, 2013; Tester & Langridge, 2010). This intensive scientific inquiry has led to the development of a variety of instruments and measurement techniques ranging widely in spaciotemporal scale to further studies of plant photosynthesis. Gas exchange is one such technique and can be monitored using O_2 electrodes or, for CO_2, infra-red gas analyzers that can quantify CO_2 flux at the ecosystem, canopy, whole-plant or leaf levels (Perdomo, Sales, & Carmo-Silva, 2018). Leaf-level CO_2 gas exchange measurements are commonly used to directly measure net CO_2 flux for both point-in-time measurements of leaf photosynthetic activity as well as for response curves. Gas exchange measurements are also the 'gold standard' to which optical techniques such as reflectance measurements are compared (Ainsworth, Serbin, Skoneczka, & Townsend, 2014; Silva-Perez et al., 2017). The basic practice of measuring plant CO_2 assimilation has existed for quite some time. Early systems generally quantified plant CO_2 uptake by flowing air from a

plant chamber through CO_2 absorbing solutions followed by titration (Heinicke & Hoffman, 1933; McLean, 1920) or conductance measurements (Spoehr & McGee, 1924; Thomas & Hill, 1937). Later systems used infra-red gas analyzers (IRGAs) which allowed for greater precision and continuous monitoring of an air stream (Mooney, 1972). The need for field measurements of photosynthetic rates led to the creation of some early mobile laboratories for this purpose (Mooney et al., 1971; Strain, 1969), although such systems were still large and difficult to get to many field sites. Given the nearly century-long history of gas exchange measurements, system requirements for accurate and precise measurements are now well understood (Bloom, Mooney, Björkman, & Berry, 1980; Long, Farage, & Garcia, 1996; Long & Hällgren, 1993; Long & Ireland, 1985), and portable commercial systems allow for routine measurement of physiologically useful parameters (Long & Bernacchi, 2003; Sharkey, 2016).

Modern commercial gas exchange systems generally follow an open path measurement principle where the system does not attempt to seal the leaf chamber or system off from all incoming air; instead, a flow of air continuously enters and leaves the chamber. Plant assimilation is then calculated from (Long & Hällgren, 1993):

$$A = \frac{u_1 c_1 - u_2 c_2}{S}, \tag{1}$$

where A is plant assimilation of CO_2 (mol m^{-2} s^{-1}), S is leaf area (m^2), u_1 and u_2 represent the incoming and outgoing air mass flow rates (mol s^{-1}) and c_1 and c_2 are the incoming and outgoing mole fraction of CO_2 in the air (mol mol^{-1}). Notably, the assimilation expression in Equation (1) assumes that steady-state conditions are present, meaning that in this case, CO_2 is stable over time. Violations of the steady-state assumption lead to errors in the calculated assimilation rate.

The steady-state paradigm has long been used as the basis for getting accurate measurements from open system gas exchange instruments. In practice, this has meant waiting for chamber stability to occur before logging data, a process that has generally required about 1–5 min, or longer depending on the application, for every data point that is logged. This steady-state requirement has had important implications for the data throughput obtainable from gas exchange systems. Recently, a Rapid A/Ci Response (RACiR) technique (Stinziano et al., 2017; Stinziano et al., 2019) was described that used a ramping CO_2 input and an empty chamber correction to obtain data that was similar to the data obtained using traditional steady-state techniques. The RACiR technique resulted in CO_2 response curves with higher data density that were also acquired over a shorter period than data obtained using traditional steady-state approaches, and the technique may be useful for getting additional insights into plant physiology as well (Lawrence, Stinziano, & Hanson, 2019; Stinziano, Adamson, & Hanson, 2019). However, concerns were raised (Taylor & Long, 2019) that RACiR may result in poor estimates for certain parameters such as the CO_2 compensation point (Γ), dark respiration (R_d) and $c_{i,trans}$, the transition point where carboxylation limitations are replaced by TPU or electron transport limitations. More work with larger data sets would likely be helpful to better investigate these issues and determine what methods, if needed, may be used to correct them (Stinziano, McDermitt, et al., 2019).

The RACiR technique provided an example of a non-steady-state technique where information about plant physiology was obtained from a leaf cuvette where conditions inside the cuvette were changing due to ramping the incoming CO_2 mole fraction. The need for an empty chamber correction arose from, firstly, the fact that the assimilation calculation (Equation [1]) assumes steady-state conditions, which were expressly violated when the leaf chamber CO_2 concentration was changing. Smaller factors, including changing IRGA match offsets as CO_2 mole fraction varied and slight flow-dependent time delays, were also corrected via the empty chamber correction. The correction itself involved fitting the empty chamber assimilation values versus reference CO_2 values with a first- to third-order polynomial over the relatively constant portion of the data set after chamber dynamics had stabilized (Stinziano et al., 2017). The empty chamber assimilation values, as a function of reference CO_2 concentration, were then subtracted from the assimilation values from CO_2 ramping experiments with plants in the leaf chamber. Thus, the RACiR technique can be described as a non-steady-state technique that requires an empirical correction.

However, another approach to non-steady-state measurements in an open system is possible that can be derived from first principles. The fundamental CO_2 mass balance for a well-mixed continuous flow leaf chamber, assuming a dry air mole fraction basis which avoids the need for a dilution correction, is given by:

$$u_1 c_1 - u_2 c_2 - sA = V\rho\frac{dc_2}{dt}, \tag{2}$$

where u_1 and u_2 represent the incoming and outgoing air mass flow rates (mol s^{-1}), c_1 and c_2 represent the incoming and outgoing CO_2 mole fractions in the air (mol mol^{-1}), s represents leaf area (m^2), A represents leaf CO_2 assimilation (mol m^{-2} s^{-1}), V represents cuvette volume (L), ρ represents air density (mol L^{-1}) and $\frac{dc_2}{dt}$ represents the rate of change of CO_2 mole fraction in the leaf chamber (mol mol^{-1} s^{-1}). A simple rearrangement, solving for assimilation, yields the following:

$$A = \frac{u_1 c_1 - u_2 c_2 - V\rho\frac{dc_2}{dt}}{s}. \tag{3}$$

The same fundamental mass balance can be applied to water vapour. Solving for transpiration and correcting for the dilution effect (where $u_2 = u_1 + sE$) yields:

$$E = \frac{u_1(h_2 - h_1) + V\rho\frac{dh_2}{dt}}{s(1 - h_2)}, \tag{4}$$

where u_1, V, ρ and s represent the same variables as defined previously, h_1 and h_2 represent the incoming and outgoing H_2O mole fractions in air (mol mol^{-1}) and E represents leaf water vapour transpiration (mol m^{-2} s^{-1}).

From Equations (3) and (4), hereafter termed the dynamic assimilation technique (DAT), it becomes clear that steady-state assimilation (Equation [1]) is simply a special case of the governing mass balance when dc_2/dt is zero. In addition, it is apparent that if incoming and outgoing CO_2 mole fractions are known with high temporal resolution

along with a good estimate of the derivative, accurate plant CO_2 assimilation values should be able to be calculated even under dynamic chamber conditions. Since the dynamic assimilation expression is general, it should also have broad applicability to numerous types of gas exchange measurements. Similarly, the dynamic expression for water vapour (Equation [4]) could result in performance gains in cases where water vapour is not steady-state, such as during survey measurements. Here, we show that implementation of the DAT is possible in a commercially available gas exchange system and that the method can be used for an array of common activities: fast CO_2 response curves from a ramping CO_2 input (similar to RACiR), faster survey measurements, and light response curves with ramping light levels. Furthermore, the method allows for the calculation of plant assimilation in real-time, thus simplifying data acquisition when compared to the RACiR technique.

2 | METHODS

2.1 | Plant material

For experiments that required plants, either soybean (*Glycine max*, cv. Karikachi) or sunflower (*Helianthus annuus*) was used. All plants were grown at a greenhouse at LI-COR Biosciences in Lincoln, NE and greenhouse temperature was maintained at 23°C–25°C. Plants were grown in a commercially available potting mixture (Miracle Gro Potting Mix, The Scotts Company LLC, Marysville, OH) and kept under well-watered conditions. Plants were between 28 and 42 days old at the time of use and in the vegetative growth phase. Plant groups were cycled such that when a given group of plants were at day 43 of their growth cycle they were replaced with a new group of plants at day 28 or 29 of their growth cycle.

2.2 | Gas exchange measurements

Gas exchange measurements were made using two LI-6800 Portable Photosynthesis Systems (LI-COR Biosciences Inc., Lincoln, NE) that were equipped with 6800-01A leaf chamber fluorometers and 6 cm^2 apertures. Version 1.3.17 and 1.4.02 of the instrument software were used for the work reported here, and system warmup tests were always run before each day's experiments per the manufacturer's recommendations. After warmup tests were completed, IRGAs were matched over a range of CO_2 concentrations, at first over several discrete steps and later using the rangematch feature. The rangematch feature ramps CO_2 and records the match offsets during the CO_2 ramp. A plot of match offsets versus sample CO_2 concentration was then fit using a polynomial and the resulting function was used to correct for match offsets between the IRGAs in real-time. This was done because point matching at various CO_2 concentrations during the ramp was not desirable and functionalizing the match offset allowed for appropriate match correction throughout the CO_2 concentration range. IRGA rangematch data were also collected at the end of experiments each day, and IRGAs were not rangematched or point-matched between individual experiments. This was done because the IRGAs were well warmed-up prior to the first CO_2 rangematch and since the instruments were always indoors they experienced little temperature variation and thus the CO_2 rangematch showed little variation over time. Had the experiments been conducted outdoors in a less stable temperature environment, the CO_2 rangematch would have needed periodic updating throughout the day. All measurements were made on the two youngest leaves (common petiole for soybean, or sequential for sunflower) that were large enough to fill the leaf chamber. Unless otherwise noted, chamber air flow was 600 μmol s^{-1}, pump setting was "auto", chamber fan mixing speed was 10,000 rpm, chamber relative humidity was controlled at 60%, chamber CO_2 was controlled at 405 ppm and chamber air temperature (Tair) was controlled at 25°C. Actinic light varied depending upon the nature of the experiment that was being conducted. Prior to running each day's experiments, the leaves were allowed to adapt to these conditions for 75–90 min.

2.3 | Empty chamber experiments

Initial validation of dynamic assimilation used empty leaf cuvettes to measure method performance under dynamic cuvette conditions against the expected flux of zero. These tests involved changing the input CO_2 mole fraction in various ways and monitoring method performance. The empty chamber experiments allowed for the development of small corrections, such as for slight time delays, where chamber or instrument behavior deviated slightly from model expectations. The required correction depended upon flow rate, which suggested that time delays rather than CO_2 adsorption or desorption were responsible for the offsets. These slight delays were accounted for by time-shifting the sample CO_2 data slightly, depending upon flow rate, such that the calculated CO_2 flux matched the expected flux value of zero.

2.4 | Steady-state CO_2 response curves

For CO_2 response curves generated using the standard steady-state methodology, the "CO_2 Response" auto-program was used to log data to the instrument. The curves were conducted using the following setpoints: 1,605, 1,405, 1,205, 1,005, 805, 605, 405, 205, 105, 55 and 5 μmol mol^{-1}. Minimum/maximum wait times were generally set to 65/65 or 70/70 s to allow for an equal amount of time at each CO_2 set point. Instrument averaging time was set to 4 s. Light levels were set to 2,000 μmol m^{-2} s^{-1}, with an 80% red and 20% blue light composition. After the auto-program was complete, chamber CO_2 was returned to the initial equilibration value.

2.5 | Dynamic assimilation and RACiR CO_2 response curves

Response curves utilizing continuous CO_2 ramps were conducted in a way similar to that of Stinziano et al. (2017) except that dynamic

assimilation curves did not require an empty chamber correction and data were logged directly to a PC, rather than to the console. Replicate CO_2 response curves occurring on the same day were always conducted on the same leaf without removing the leaf from the leaf chamber to minimize the effects of biological variability when comparing the steady-state, RACiR and dynamic assimilation methods. Thus, both steady-state and continuous CO_2 ramping response curves were conducted on the same leaf each day to facilitate comparisons between methods. For experiments comparing RACiR and dynamic assimilation, the CO_2 ramping rate was limited to 100 μmol mol^{-1} s^{-1} in accordance with recommending best practices (Stinziano, McDermitt, et al., 2019). In these experiments, an empty chamber data set was collected before the CO_2 response curve for data correction purposes. To generate the correction equation needed for RACiR, the empty chamber CO_2 assimilation data were regressed against reference CO_2 using a third-order polynomial in accordance with previous work (Stinziano et al., 2017). Also, the RACiR and dynamic assimilation results were computed from the same exact CO_2 response curve data set to facilitate the best possible comparison. Between all response curves, leaves were allowed to equilibrate 60–75 min in the leaf chamber to ensure the leaf was able to return to steady-state conditions. CO_2 ramps, using reference CO_2, were set up using the 'Auto Controls' feature of the instrumentation software. CO_2 ramps were run from 1,605 to 5 μmol mol^{-1} or 5 to 1,605 μmol mol^{-1} using ramping rates of 100, 200, or 400 μmol mol^{-1} min^{-1} which led to a total running time of 16, 8, and 4 min for the CO_2 ramps, respectively. Prior to starting a CO_2 ramp, water vapour was set to reference control using the same water vapour mole fraction the instrument was using to maintain chamber relative humidity at 60%; after completion of a CO_2 ramp, water vapour control was set to maintain chamber relative humidity at 60%. Reference CO_2 was then set to the initial ramping CO_2 concentration and, about 5–10 s after reference CO_2 reached the target, data collection was initiated and 60 s of data were collected before starting the CO_2 ramp. In cases where oscillations in assimilation were observed, it was necessary to wait 1–4 min until the oscillations were dampened before starting the CO_2 ramp. After completion of a CO_2 ramp, an additional 60 s of data were collected and then chamber CO_2 was returned to 405 μmol mol^{-1}.

2.6 | Steady-state light response curves

For light response curves that used the steady-state methodology, the "Light Response" auto program was used to conduct the curve and log data to the instrument. For full light response curves, the actinic light values were set to 2,000, 1,867, 1,733, 1,600, 1,467, 1,333, 1,200, 1,067, 933, 800, 667, 533, 400, 267, 133 and 10 μmol m^{-2} s^{-1}. For quantum yield determination, the actinic light flux values used were 120, 108, 96, 84, 72, 60, 48, 36, 24, 12 and 0 μmol m^{-2} s^{-1}. Minimum and maximum wait times were both set to 120 s, which resulted in the light response program spending an equal amount of time at each point in the curve. Sample CO_2 was controlled at 400 or 405 μmol mol^{-1}. After the program was finished, the actinic light was returned to its starting value.

2.7 | Non-steady-state light response curves

These experiments ramped actinic light to generate light response data over time. In all cases, plants were allowed to light adapt to either 2,000 or 120 μmol m^{-2} s^{-1} actinic light and reach steady-state conditions prior to starting a light ramp. The chamber actinic light was ramped from 2,000 to 0 μmol m^{-2} s^{-1} for 30 or 40 min or, for quantum yield determination, from 120 to 0 μmol m^{-2} s^{-1} for 20 min. Sample CO_2 was controlled at 400 or 405 μmol mol^{-1}. Data were directly logged to a PC as previously described at 2 Hz. After a light ramp was complete, the actinic light was returned to its starting value.

2.8 | Survey measurements

Experiments to determine the utility of dynamic assimilation for survey measurements were conducted using empty chamber tests and light-adapted plants. Empty chamber tests focused on how quickly the assimilation value returned to zero after the leaf cuvette was opened and subsequently closed. Tests done using a leaf monitored the performance of both steady-state and dynamic assimilation after the leaf cuvette was closed on a light-adapted leaf and the time required for both methods to reach a stable assimilation value. For these tests, air flow was set to 600 μmol s^{-1}, CO_2 was controlled at 420 μmol mol^{-1} using the reference IRGA, moisture was controlled on reference mole fraction at 24 mmol mol^{-1}, the temperature was controlled at ambient on exchanger temperature, and actinic light was set to match leaf-level PAR as measured by the on-board PAR sensor placed next to the leaf immediately before assimilation measurement. Data were logged to a computer as previously described.

2.9 | Data processing and analysis

Data from non-steady-state experiments were logged to a PC (Dell XPS 139370, Dell Inc., Round Rock, TX) at 2 Hz from the LI-6800 and initially sorted using a custom macro in Microsoft Excel (version 1902, Microsoft Inc., Redmond, WA) so that the data could be imported into other programs. GNU Octave version 4.4.1 (Eaton, Bateman, & Hauberg, 2018) was used for the computation of dynamic assimilation using Equation (3). The Octave script averaged the data, applied a matching adjustment of the sample CO_2 mole fraction, calculated the leaf chamber CO_2 mole fraction derivative and adjusted for small-time delays. An example Octave script is provided (see Supporting information). For mass balance simulation purposes, the Octave 'lsode' ODE solver was used to solve Equation (2) for c_2. The equation assumed an empty leaf chamber with an assimilation rate of zero, and was parameterized using a ramping CO_2 vector from 5 to 2,005 μmol mol^{-1} at 200 μmol mol^{-1} min^{-1} for c_1 and used the same chamber volume and

air density that was present during the empty chamber experiments. Once c_2 was solved for the difference between c_1 and c_2 in the model was calculated. For light response curves, a leaf absorptance value of 0.85 was assumed. Curve fitting and parameter estimates for CO_2 response curves were generated using R version 3.6.2 (R Core Team, 2019) and the 'plantecophys' package (Duursma, 2015). To estimate $V_{c,max}$ and J_{max}, CO_2 response curve data were fit using data where C_i < 500 μmol mol^{-1} except where noted to avoid fitting data where TPU limitation appeared to be present. All settings in the 'fitaci' function were left at their respective default values, and the default nonlinear fitting method was used, which allowed for the calculation of reliable standard errors. In all cases, the fitting method was able to satisfy the default convergence criteria and generate parameter estimates. Parameter standard error estimates were from the curve fit results table in R and 95% confidence intervals for parameters were derived using the 'confint' procedure in R.

3 | RESULTS

3.1 | Empty chamber tests

Since an empty leaf chamber should always have a flux value of zero, tests done using an empty chamber were a useful way of evaluating the implementation of the non-steady-state equation (Equation [3]). Results from an empty chamber experiment are shown in Figure 1a, b, where CO_2 was ramped from 5 to 2,005 μmol mol^{-1} at a rate of 200 μmol mol^{-1} min^{-1}. Dynamic assimilation remained near zero throughout the CO_2 ramp while steady-state assimilation showed the expected offset. The mean CO_2 assimilation value for dynamic assimilation was 0.06 ± 0.48 μmol m^{-2} s^{-1} while the mean steady-state CO_2 assimilation value, between 150 and 650 s, was 20.38 ± 0.37 μmol m^{-2} s^{-1}. Results from another test, using a sawtooth-shaped CO_2 input over time are shown in Figure 1c,d. The

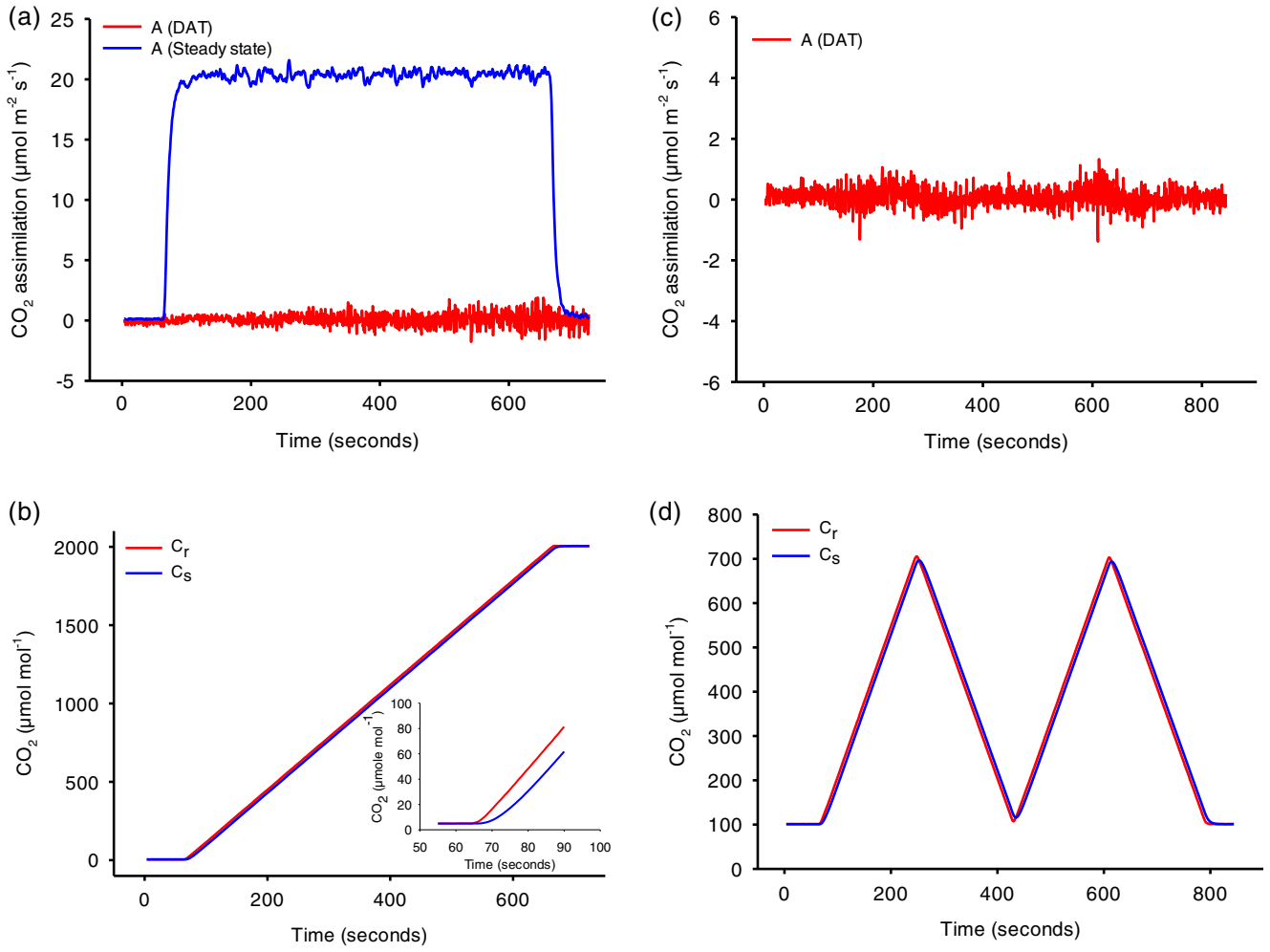

FIGURE 1 Comparison of dynamic and steady-state methods. (a) In an empty 6800-01A chamber, dynamic assimilation and steady-state assimilation are compared when the incoming air CO_2 is changing over time. (b) Diagram showing the change in CO_2 over time in the system reference and sample IRGAs. The inset graph shows reference and sample CO_2 at the time of CO_2 ramp initiation. (c) Dynamic assimilation results when chamber input CO_2 is ramped up and down in a repeating sawtooth pattern, as shown in (d)

mean value for dynamic CO_2 assimilation in this test was 0.08 ± 0.31 μmol m^{-2} s^{-1}.

Another validation of the DAT involved simulating the mass balance to establish a baseline with which to compare empty chamber data. The model (Equation [2]) was solved numerically as described in the methods section assuming an empty chamber with an assimilation rate of zero. From the model output results, the difference between c_1 and c_2 were calculated. These results were compared to data obtained with the LI-6800 using the same CO_2 ramping rate as the simulation (200 μmol mol^{-1} min^{-1}) and ΔCO_2 values were calculated from the difference between the sample (C_s) and reference (C_r) IRGAs from the LI-6800 data. Results of this comparison are shown in Figure 2, where the LI-6800 data shows close agreement with model output, which suggested the system conformed well to the expectations of the theoretical model. Ramping CO_2 inputs were also tested using various system flow rates and results are shown in Table 1. In general, mean assimilation values were close to the expected value of zero, although higher flow rates, as well as the higher CO_2 ramping rate, tended to show a larger offset from zero. Based on the empty chamber tests, a flow rate of 600 μmol s^{-1} was selected for all additional testing.

3.2 | CO_2 response curves

One of the primary goals during method development was to assess the viability of dynamic assimilation non-steady-state methodology for CO_2 response curves. In particular, the performance of the method using faster CO_2 ramping rates than currently recommended for RACiR (Stinziano, McDermitt, et al., 2019) was of interest to potentially further reduce the time required to obtain CO_2 response curve

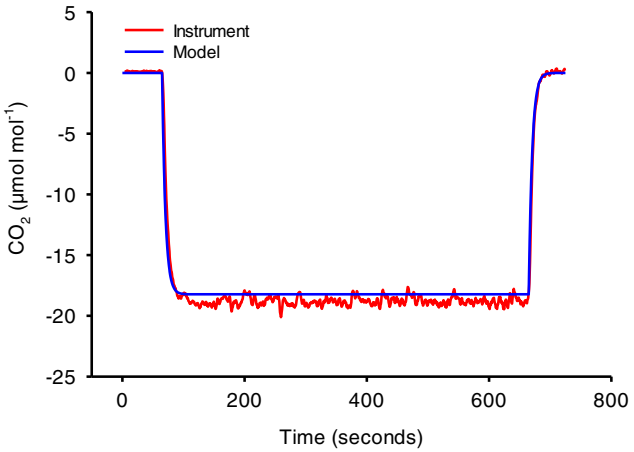

FIGURE 2 Comparison of instrument behavior to theoretical model output under empty chamber conditions. A flow rate of 600 μmol s^{-1} was used with a 5–2,005 μmol mol^{-1} CO_2 ramp. For the instrument, ΔCO_2 was calculated from the difference between sample (Cs) and reference (Cr) CO_2. For the model, ΔCO_2 was calculated from the difference between c_2 and c_1 [Colour figure can be viewed at wileyonlinelibrary.com]

data. The CO_2 ramps used to generate the data in Figure 3a were from 1,605 to 5 μmol mol^{-1} for 16 or 8 min, reflecting the CO_2 ramping rates of 100 and 200 μmol mol^{-1} min^{-1}. Figure 3b magnifies data from Figure 3a near the CO_2 compensation point. The CO_2 ramps used for Figure 3c were from 1,605 to 5 μmol mol^{-1} and occurred for 8 and 4 min, reflecting the CO_2 ramping rates of 200 and 400 μmol mol^{-1} min^{-1}. Figure 3d magnifies data from 3C near the CO_2 compensation point. Frequently, when leaf cuvette concentration was changed from 405 to nearly 1,605 μmol mol^{-1}, oscillatory behavior in leaf CO_2 assimilation was observed (data not shown). In such cases, the CO_2 ramp was not started until the oscillations disappeared, which generally required 1–4 min. Curve fit results comparing dynamic assimilation to RACiR and the traditional steady-state method are shown in Table 2. Graphical results from the curve fits are shown in Figure S1. The RACiR results were computed from the same data set that the 100 μmol mol^{-1} min^{-1} dynamic assimilation results used. The resulting parameter estimates for $V_{c,max}$ and J_{max} showed generally good similarity across methods, although the RACiR method yielded a lower estimate for the calculated parameters and the RACiR CO_2 compensation point was also lower (Figure 3b) when compared to the dynamic assimilation results. Parameter uncertainty from the CO_2 ramping methods was smaller by a factor of about 3 to over an order of magnitude for both $V_{c,max}$ and J_{max} and, as a result, the 95% confidence intervals for the dynamic assimilation and RACiR parameter estimates were substantially smaller as well.

CO_2 ramps were also conducted that were monotonically increasing from 5 to 1,605 μmol mol^{-1}. For these ramps, generally similar results were obtained as for the monotonically decreasing ramps (1,605–5 μmol mol^{-1}) described above. However, differences were sometimes observed in these ramps that were not seen in the monotonically decreasing ramps. For one, oscillations in assimilation as previously described were not present. For another, an apparent assimilation peak followed by a relatively rapid decline was frequently, though not always observed as seen in Figure 4a. This feature could also be observed when the CO_2 ramp started at ambient CO_2 and was monotonically increased from 405 to 2,000 μmol mol^{-1} (Figure 4b), suggesting it was not caused by leaf exposure to low CO_2 concentrations and potential Rubisco deactivation. Although TPU limitation may have been present in some of the monotonically decreasing CO_2 ramps (see Figure 3a), no such ramp revealed the relatively rapid decrease in assimilation between C_i values of about 450–700 μmol mol^{-1} as seen in Figure 4a,b.

3.3 | Light response curves

Since dynamic assimilation can correctly calculate assimilation when chamber conditions violate steady-state assumptions, several experiments were conducted to determine the suitability of this technique for obtaining accurate light response curve data. In this case, the goal was to produce curves with higher data density than is typical for traditional steady-state techniques. Results from a typical light response curve from soybean are shown in Figure 5, which shows steady-state

TABLE 1 Empty chamber testing results over two CO_2 ramping rates and several system flow rates

CO_2 ramping rate (μmol mol^{-1} min^{-1})	Flow rate (μmol s^{-1})	Mean A (overall)[a] (μmol m^{-2} s^{-1})	Mean A (ramp)[a] (μmol m^{-2} s^{-1})
200	300	0.15 ± 0.51	0.17 ± 0.47
	400	−0.09 ± 0.50	−0.13 ± 0.47
	500	0.30 ± 0.48	0.38 ± 0.46
	600[b]	0.33 ± 0.50	0.37 ± 0.48
	700	0.40 ± 0.53	0.51 ± 0.48
	800	−0.92 ± 0.56	−1.04 ± 0.50
	900	−0.23 ± 0.50	−0.24 ± 0.47
400	300	0.29 ± 0.74	0.28 ± 0.60
	400	−0.09 ± 0.72	−0.23 ± 0.57
	500	0.73 ± 0.67	0.98 ± 0.53
	600[b]	0.38 ± 0.55	0.47 ± 0.48
	700	1.10 ± 0.79	1.50 ± 0.54
	800	−0.98 ± 0.83	−1.39 ± 0.57
	900	−0.15 ± 0.50	−0.17 ± 0.51

Note: The overall mean represents data over the entire experiment, which includes periods when CO_2 is stable. The ramping mean represents the average assimilation value during the CO_2 ramp.

[a]Error term represents the standard deviation of the data.

[b]Raw data from these experiments is available in supporting information.

and dynamic assimilation data. The data shows good agreement between the two methods, which was not surprising since the instrument was set to keep chamber CO_2 relatively constant at 405 μmol mol^{-1} which thereby kept the contribution from the derivative term low as well. However, quantitative determinations of the quantum yield and light compensation point were problematic from these experiments because of insufficient data density from the steady-state technique resulting in parameter estimates with a large associated error. Therefore, experiments designed to compare quantitative values, namely the quantum yield (ϕ) and light compensation point, were conducted using sunflower. Results of a typical experiment are shown in Figure 6a, where steady-state and dynamic assimilation experiments were conducted over identical 20-min time scales and used identical actinic light profiles over time (Figure 6b). Stomatal conductance values were also very similar between the experiments (Figure 6c). Quantum yield determinations were 0.0639 (95% CI: 0.0637, 0.0642) and 0.0635 (95% CI: 0.0617, 0.0652) for the dynamic assimilation and steady-state methods, respectively, which were reasonable since photorespiration was not being suppressed in these experiments. The light compensation points were calculated to be 18.8 and 20.9 μmol m^{-2} s^{-1} for the dynamic and steady-state method, respectively.

3.4 | Survey measurements

Several empty chamber tests were conducted to compare how fast the dynamic and steady-state assimilation techniques would return to the expected value of zero. Results from a typical experiment are shown in Figure 7a. At 30s, the leaf chamber was opened for 10 s. At approximately 40 s, the leaf cuvette was closed, causing a spike in assimilation values as chamber washout occurred. As seen in Figure 7a, the dynamic assimilation values reached zero faster than the steady-state assimilation values by over 15 s, suggesting the possibility for reduced time requirements for survey measurements. Dynamic calculations for transpiration compared to steady-state transpiration values are shown in Figure 7b. Further testing using sunflower showed dynamic assimilation resulted in a reduced time required to reach stability as well. Data from a typical experiment is shown in Figure 7c, where the leaf cuvette was first closed, then opened and clamped on to a leaf. The data showed that, within approximately 10 s of chamber closure, dynamic assimilation had stabilized and remained relatively constant while steady-state assimilation required about 20 more seconds to reach a stable value. A comparison of dynamic and steady-state transpiration is shown in Figure 7d. In this case, transpiration calculated on a dynamic basis (Equation [4]) was able to approach stability faster than steady-state transpiration, but the difference between the dynamic and steady-state forms was smaller than for CO_2 assimilation. Dynamic transpiration was then used in the calculation of stomatal conductance to water vapour (g_{sw}). A comparison of stomatal conductance to water vapour calculated on a dynamic and steady-state basis is shown in Figure 7e; the data followed a similar trend to the transpiration results in that the dynamic form approached stability faster than the steady-state calculation.

4 | DISCUSSION

Plant gas exchange measurement is a well-established technique that provides insight into several important physiological parameters, such as CO_2 assimilation and stomatal conductance. These measurements,

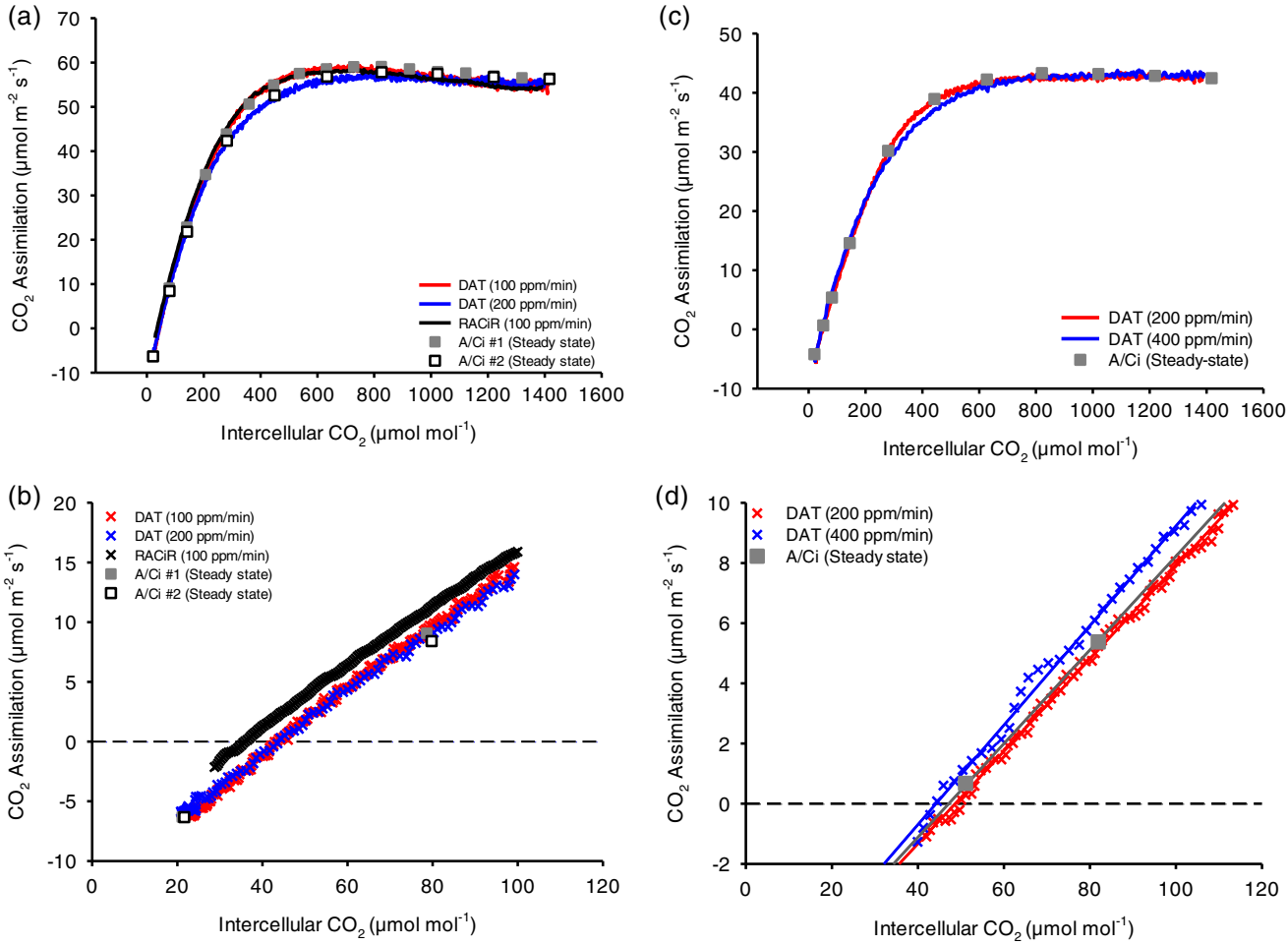

FIGURE 3 Comparison of dynamic assimilation and CO_2 ramps and traditional steady-state methods for generating the A/Ci response curves. (a) Full-scale response curves in sunflower show broadly similar results between the dynamic and steady-state techniques. CO_2 was ramped from 1,605 to 5 µmol mol^{-1} at either 100 or 200 µmol mol^{-1} min^{-1}. RACiR calculations were done using data from the 100 µmol mol^{-1} min^{-1} ramping rate. (b) Showing a subset of the data in Figure 3a near the CO_2 compensation point. The dynamic photosynthesis method clusters well with the steady-state technique, while the RACiR method appears to underestimate the compensation point. (c) Full-scale CO_2 response curve in sunflower utilizing CO_2 ramping rates of 200 or 400 µmol mol^{-1} min^{-1} compared to a steady-state CO_2 response curve. (d) Showing a subset of the data in Figure 3c near the CO_2 compensation point. Data from Figure 3a is included in supporting information [Colour figure can be viewed at wileyonlinelibrary.com]

while being non-destructive and very useful for understanding plant physiology, have been subject to the relatively long time requirements for obtaining a good measurement. This time requirement has also precluded gas exchange measurements from high throughput applications (Fu, Meacham-Hensold, Guan, & Bernacchi, 2019), despite the utility gas exchange measurements could provide in such scenarios. These time requirements are, in turn, a function of both instrumentation design and the underlying theoretical principles on which the calculation of variables rely. Instrumentation design factors include flow path, flow rates, IRGA placement and sensitivity, temperature measurement and leaf cuvette design. Leaf cuvettes for small leaf surface areas can present problems of edge effects and leakage rates; furthermore, the small area measured may not represent a good spatial average of the leaf under study. Large leaf cuvettes present challenges that include achieving adequate environmental control, sufficient air mixing and slow response times.

For systems with an open flow path design, a limitation that imposes a time restriction is the requirement of steady-state. In particular, steady-state requires the presence of stable cuvette CO_2 concentrations before assimilation can be accurately computed. This means that a period must elapse, based on residence time distribution characteristics of the leaf cuvette, before the accurate steady-state measurement is possible even when leaf assimilation is stable and not responding to a change in environmental conditions. Steady-state requirements do not necessarily preclude fast measurements since systems designed for fast measurement of plant gas exchange have been developed (Laisk & Oja, 1998). However, steady-state conditions are not a prerequisite for measuring leaf assimilation in an open path system. From a CO_2 mass balance of a leaf cuvette, we have shown that the steady-state condition is simply a special case of the general mass balance when the derivative is zero. We implemented a general mass balance on data gathered from a commercially available gas

TABLE 2 Parameter estimates from fitting the data shown in Figure 3 to the FvCB model of photosynthesis

Experiment	$V_{c,max}$[a] (μmol m^{-2} s^{-1})	95% CI	J_{max}[a] (μmol m^{-2} s^{-1})	95% CI	R_d (μmol m^{-2} s^{-1})	95% CI
Parameter estimates below are from Figure 3a data						
DAT (100 μmol mol^{-1} min^{-1})	204.4 ± 0.4	(203.4, 205.4)	369.2 ± 0.7	(367.8, 370.6)	0.38 ± 0.06	(0.26, 0.50)
DAT (200 μmol mol^{-1} min^{-1})	194.9 ± 0.6	(193.5, 196.4)	337.2 ± 0.9	(335.3, 339.0)	0.55 ± 0.08	(0.39, 0.71)
RACiR (100 μmol mol^{-1} min^{-1})	195.3 ± 0.40	(194.4, 196.2)	347.0 ± 0.6	(345.9, 348.2)	−2.0 ± 0.05	(−2.1, −1.9)
A/Ci #1[b] (steady-state)	201.6 ± 4.7	(189.4, 218.0)	371.9 ± 8.1	(351.6, 393.4)	0.56 ± 0.6	(−1.1, 2.2)
A/Ci #2[c] (steady-state)	192.1 ± 4.2	(178.8, 218.3)	354.8 ± 6.9	(333.6, 377.4)	0.97 ± 0.5	(−0.75, 2.7)
Parameter estimates below are from Figure 3c data						
DAT (200 μmol mol^{-1} min^{-1})	138.0 ± 0.20	(137.6, 138.4)	244.2 ± 0.3	(243.5, 244.8)	1.95 ± 0.02	(1.9, 2.0)
DAT[d] (400 μmol mol^{-1} min^{-1})	132.1 ± 0.5	(131.0, 133.3)	234.0 ± 0.6	(232.9, 235.1)	1.18 ± 0.06	(1.1, 1.3)
A/Ci[e] (steady-state)	133.2 ± 1.6	(128.8, 137.6)	241.4 ± 2.0	(235.8, 247.0)	0.91 ± 0.2	(0.39,1.4)

Note: Parameter estimates, errors, and 95% confidence intervals (CI) were generated using R and the 'plantecophys' package (Duursma, 2015). The default parameter settings were used for the 'fitaci' function. $V_{c,max}$ and J_{max} were scaled to 25°C, Patm = 100, $\alpha = 0.24$, $\Theta = 0.85$, EaV = 82,620.87, delsC = 645.1013, EaJ = 39,676.89, EdVJ = 2e5 and delsJ = 641.3615. Any parameter or function option not listed here was set to the default value. Data passed to the 'fitaci' function included leaf CO_2 assimilation, C_i, leaf temperature and leaf PPFD. R_d was estimated from the data rather than specified prior to fitting. Model fits used gas exchange data with C_i < 500 μmol mol^{-1} unless otherwise noted.

[a]Error term represents the standard error of the parameter fit reported by R.

[b]Included data at C_i = 536.5 μmol mol^{-1}.

[c]Included data at C_i = 633.5 μmol mol^{-1}.

[d]Included all C_i < 800 μmol mol^{-1}.

[e]Included data at C_i = 626.8 μmol mol^{-1}.

exchange instrument to see if accurate measurements could be obtained under non-steady-state cuvette conditions using some typical scenarios for which gas exchange is used.

Initial experiments using empty leaf chambers suggested dynamic assimilation could meet theoretical expectations. For well-mixed, continuous flow systems, when a ramping input of a chemical species is input into such a system, a concentration difference will become established between the input concentration and the tank or chamber concentration even if no reaction is taking place. In the case of a gas exchange system with an empty leaf chamber, this results in a concentration difference between the reference and sample IRGAs which results in an apparent assimilation value during the CO_2 ramp when calculated on a steady-state basis. The exact apparent assimilation value will vary, depending upon the direction of the CO_2 ramp and properties of the system. This is the primary reason that the RACiR technique requires an empty chamber correction. However, when CO_2 assimilation is calculated on a dynamic basis, the assimilation value should remain near the true value of zero. The results from empty chamber experiments demonstrated that dynamic assimilation was able to achieve this result. Model simulations, using numerical techniques to solve Equation (2) for c_2, showed good agreement between the expected concentration difference between c_1 and c_2 and the actual difference between reference CO_2 (Cr) and sample CO_2 (Cs) that was observed in the gas exchange system. This suggested that the CO_2 dynamic mass balance was a good model for the gas exchange system.

Similar to steady-state measurements, limitations to dynamic assimilation also exist. More noise was evident in the dynamic CO_2 assimilation results. This was likely due to a combination of factors. For one, less averaging was used. Steady-state measurements reported here used a 4 s average while the dynamic measurements used a 3 s average. Also, numerical differentiation is an inherently noisy numerical process that amplifies noise in the implementation of the dynamic mass balance; higher CO_2 concentrations also show slightly more noise due to fixed limits of analog-to-digital conversion and the shape of the underlying calibration curve. Taken together, more noise is expected when comparing dynamic to steady-state calculations, but the increase in the amount of data obtained offsets this effect. CO_2 ramping rates likely present another potential limitation from either an instrument or biological standpoint. Here, CO_2 response curves utilized CO_2 ramping rates of up to 400 μmol mol^{-1} min^{-1}. Faster ramping rates may be possible but will need further validation. At some point, instrument control capability limits may be reached which could introduce error into the calculated assimilation rates. Insufficient data sampling and logging rates could also prove to limit in cases where chamber conditions change too rapidly. Finally, if a leaf chamber is not carefully designed, poor mixing or adsorption/desorption effects could bias or lead to error in the results. Commercial systems are generally designed to provide good mixing and minimize adsorption, but custom or laboratory-built chambers may be more variable. For the chamber used here, the 6800-01A, CO_2 adsorption did not appear to meaningfully influence the results. Finally, leaves with low assimilatory flux values present similar challenges for both dynamic and steady-state measurements. Fundamentally, measuring assimilation requires developing a resolvable CO_2 difference outside of the instrument noise that low assimilatory fluxes may not achieve. In these cases, lowering the air flow rate into the leaf chamber should help increase the CO_2 differential.

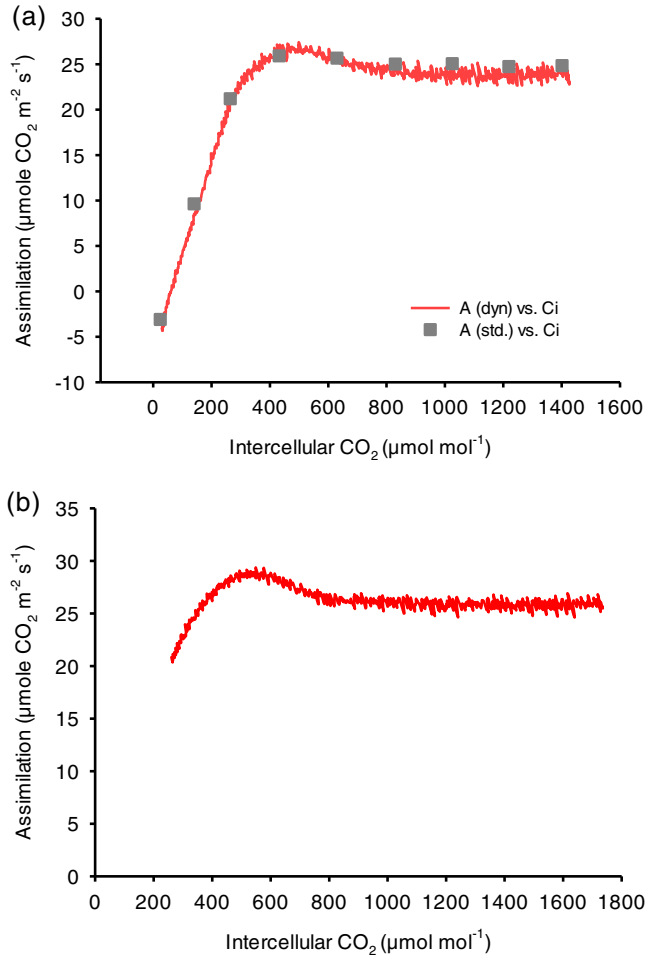

FIGURE 4 (a) The dynamic assimilation method more clearly resolves an apparent assimilation overshoot than is observed with the steady-state method. (b) Results from a 430 to 2,000 µmol mol^{-1} CO_2 ramping experiment in soybean showing the assimilation overshoot can be present even without prior exposure to low CO_2 levels [Colour figure can be viewed at wileyonlinelibrary.com]

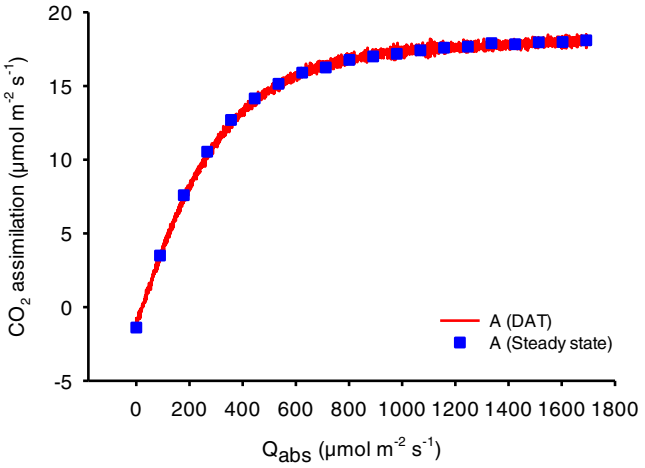

FIGURE 5 Comparison of dynamic and steady-state methods for an A-Q curve using soybean. For the dynamic method, actinic light was ramped from 2,000 to 0 µmol m^{-2} s^{-1} over 40 min. The steady-state method changed the actinic light level every 2 min [Colour figure can be viewed at wileyonlinelibrary.com]

The results show that dynamic assimilation may hold some advantages over the traditional steady-state technique. For CO_2 response curves, dynamic assimilation produced results substantially similar to those obtained from steady-state response curves. In response curves that used a CO_2 ramp, the dynamic formulation only changed the way assimilation was calculated; transpiration was calculated using steady-state equations. Water vapour relationships tend to change slowly during a dynamic or steady-state CO_2 response curve as the stomates open or close in response to CO_2, meaning that water vapour remains at or very near steady-state conditions during the response curve, and therefore steady-state transpiration values can be used in calculating conductance values. The results show that using the dynamic assimilation values in the calculation of C_i resulted in CO_2 response curves that agreed well with steady-state measurements. In nearly all cases, dynamic assimilation parameter estimates from sunflower showed that $V_{c,max}$ and J_{max} were indistinguishable from parameters from the steady-state response curves (Table 2) based on the overlap of the parameter 95% confidence intervals. Additionally, the dynamic assimilation results suggested that the tested CO_2 ramping rates (100, 200, and 400 µmol mol^{-1} min^{-1}) resulted in substantially similar parameter estimates. The implication is that, at least for some species, a full-range CO_2 response curve can be obtained in about 5–10 min, depending upon the CO_2 ramping rate. The RACiR results, which were computed from the same 100 µmol mol^{-1} min^{-1} CO_2 ramping data set that was used to generate the dynamic assimilation results, showed differences when compared to the dynamic assimilation results. The RACiR parameter estimates for $V_{c,max}$ and J_{max} were about 5% and 7% lower, respectively, than the 100 µmol mol^{-1} min^{-1} DAT results and did not fall within the DAT confidence intervals. Also, the apparent CO_2 compensation point from RACiR was lower than the steady-state and dynamic assimilation results as seen in Figure 3b. Finally, the RACiR curve fit returned a negative estimate for R_d, while the all the DAT curve fits estimated positive values for R_d. Steady-state curve fits also returned positive R_d estimates, although the associated uncertainty was larger. The reasons for these differences are unclear, although the uncertainty present in the steady-state curves due to the lower data density inherent in the steady-state technique prevents concluding that the RACiR results were meaningfully different from the steady-state results. However, it has also been suggested that RACiR may poorly estimate some parameters (Taylor & Long, 2019) such as the CO_2 compensation point; further work with larger data sets using the recommended best practices would better clarify this issue.

In addition to increased speed, new insights may also be possible with CO_2 ramping techniques. For instance, using the RACiR technique, multiple CO_2 ramping rates were used to investigate observed offsets between steady-state and RACiR CO_2 response curves and derive a novel estimate for Γ (Stinziano, Adamson, & Hanson, 2019). Others have used RACiR to investigate drought response in peanuts

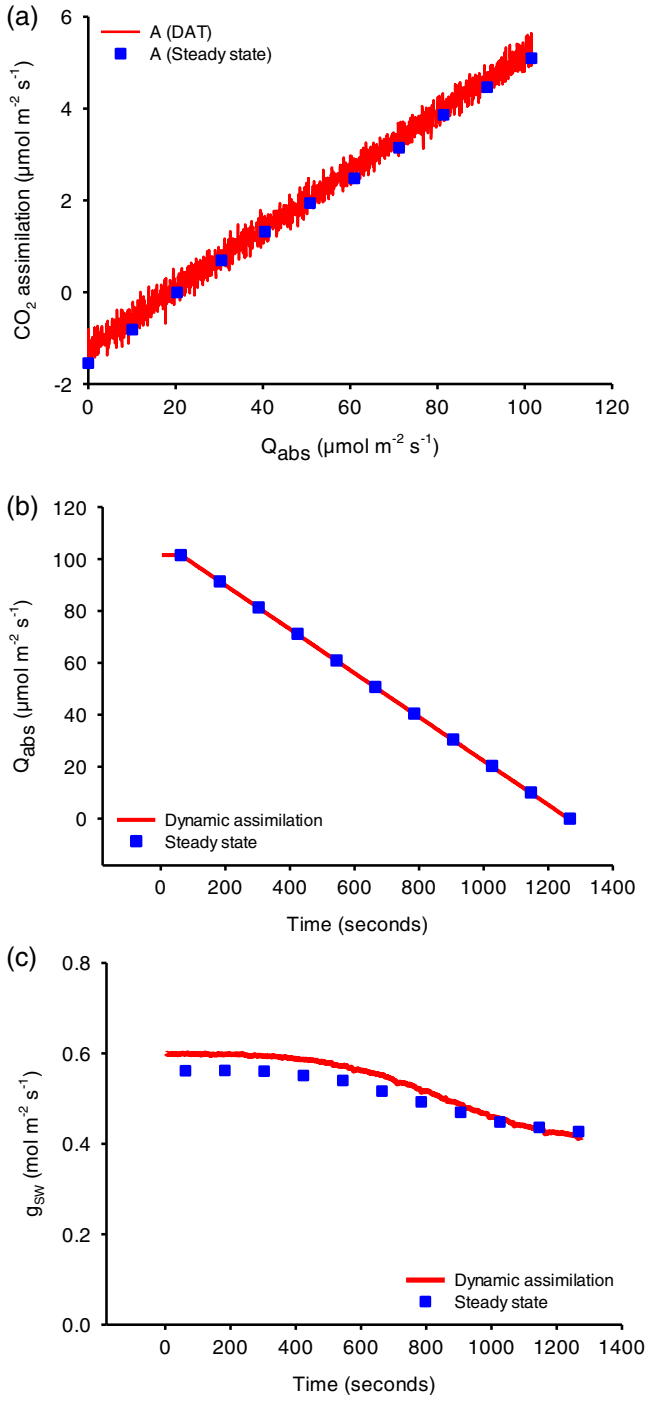

FIGURE 6 Comparison of A-Q curves for quantum yield determination using dynamic and steady-state methods. (a) Method comparison showing results from an experiment to determine quantum yield in sunflower. The dynamic assimilation method ramped actinic light from 120 to 0 µmol m^{-2} s^{-1} over 20 min. The steady-state method used 120 s per step. (b) Comparison of actinic light settings over time. (c) Comparison of stomatal conductance between the experiments [Colour figure can be viewed at wileyonlinelibrary.com]

(Pilon et al., 2018) and the technique has been expanded for use in larger leaf cuvettes in a study of balsam fir and black spruce (Coursolle, Otis Prud'homme, Lamothe, & Isabel, 2019). In this work, we note that CO_2 ramp direction in soybean can result in different features being resolved in the dynamic assimilation A/Ci curve. In particular, monotonically increasing CO_2 ramps from 5 to 1,605 ppm often, though not always, resulted in an assimilation peak followed by a relatively rapid decrease generally in the region where C_i was between 400 and 700 µmol mol^{-1}. This behavior suggested that assimilation was being limited by an effect such as TPU (Sharkey, 2019) or some other type of limitation. The fact that this feature could be observed even when leaves were not exposed to low cuvette CO_2 levels (such as during a 430–2,000 µmol mol^{-1} CO_2 ramp, Figure 4b) should preclude any influence from rubisco deactivation or temporary assimilation overshoot due to accumulation of high RuBP pools (von Caemmerer, 2000). However, further work is needed to better elucidate the mechanism(s) behind this behavior. For CO_2 ramps that were monotonically decreasing from high to low CO_2, oscillations in assimilation were frequently observed when CO_2 partial pressure was increased from ambient to saturating values of 1,605 or 2,005 µmol mol^{-1}. These oscillations always dampened over time and generally disappeared after about 1–4 min, after which the CO_2 ramp was initiated. Oscillatory behavior in assimilation has been previously observed (Laisk & Walker, 1986; Sharkey et al., 1986) and was predicted by a photosynthetic model (Laisk & Walker, 1986), and could be due to temporary imbalances in phosphate metabolism.

Another potential advantage of using high data density techniques is the improvement in parameter resolution due to the reduction in parameter uncertainty that is possible by having more data available for curve fitting. The Farquhar-von Caemmerer-Berry (FvCB) model of photosynthesis (Farquhar, von Caemmerer, & Berry, 1980; von Caemmerer, 2000) has been commonly used to derive useful parameters from CO_2 response (A/C_i) curves. However, these change-point models are nonlinear in the parameters and over-parameterized, and present challenges in fitting for obtaining good parameter estimates (Gu, Pallardy, Kevin, Law, & Wullschleger, 2010). Additionally, it has been noted that parameter accuracy is directly dependent upon both the number of data points as well as the accuracy of the underlying gas exchange data; small and noisy data sets can be particularly problematic when trying to obtain robust parameter estimates (Sharkey, Bernacchi, Farquhar, & Singsaas, 2007; Wang et al., 2017). The choice of fitting method has also been shown to impact the estimated parameter values (Miao, Xu, Lathrop Jr., & Yufei, 2009; Wang et al., 2017), which further complicates efforts to estimate accurate parameters from A versus C_i or A versus C_c curves. Often, the uncertainty associated with a parameter estimate may be reported, but the impact of this uncertainty is frequently not discussed: higher uncertainty broadens the confidence intervals, making statistical inferences of any actual differences, if they exist, more difficult or even impossible to resolve. Averaging parameters, such as done by Miao et al. (2009), can be particularly impacted by the magnitude of the parameter uncertainty if appropriate error propagation techniques are used when deriving the uncertainty associated with an averaged parameter value. Here, only a single fitting method using R and the 'plantecophys' package (Duursma, 2015) was chosen because it was readily available, well documented, and could accommodate

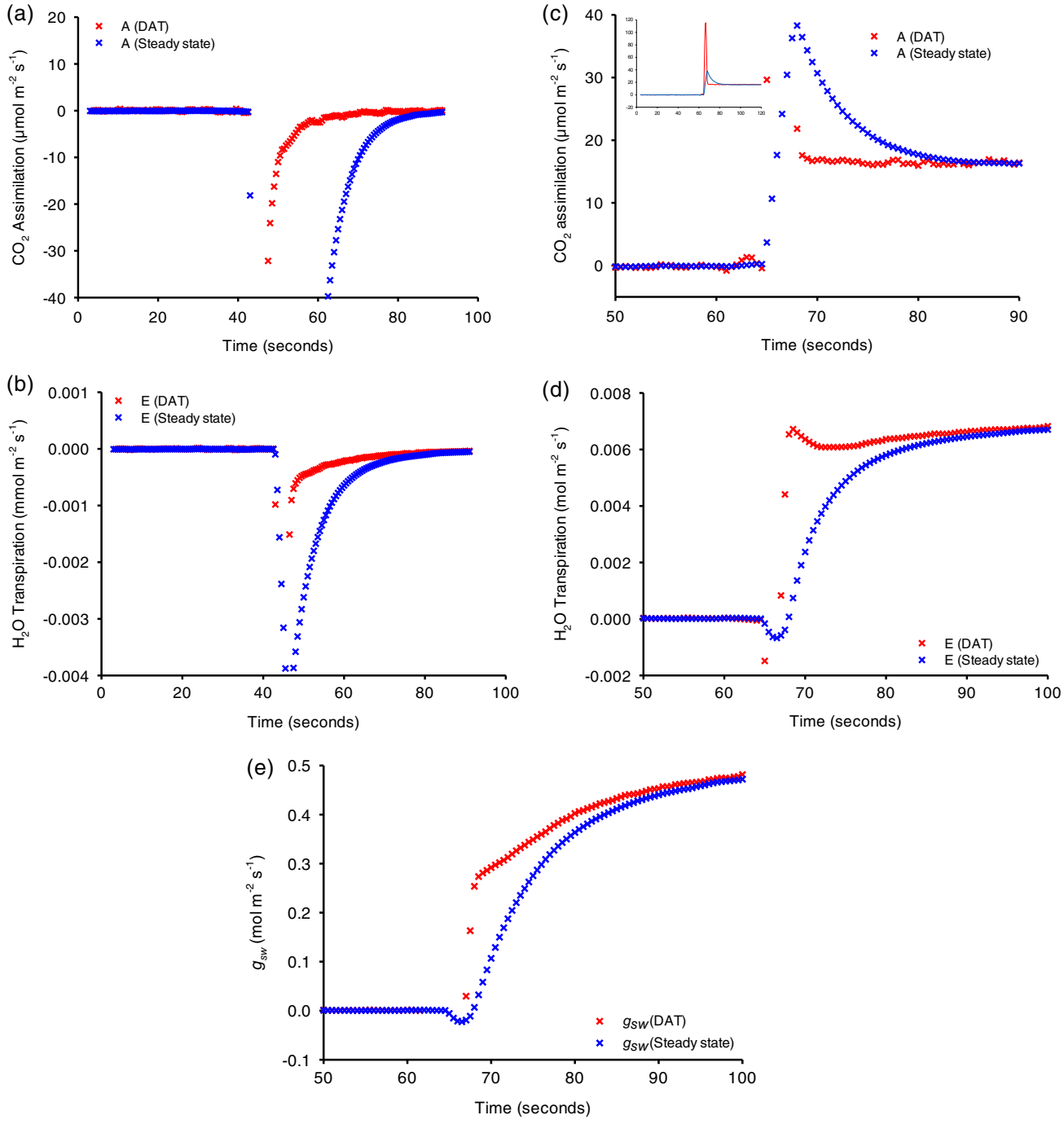

FIGURE 7 Comparison of dynamic and steady-state assimilation techniques under survey measurement conditions. (a) Method comparison using an empty chamber. The chamber was opened for approximately 10 s then closed. Dynamic assimilation returned to the expected value of zero more quickly than steady-state assimilation. (b) Data are from the same empty chamber experiment shown in Figure 6a. Transpiration calculated on a dynamic basis (Equation [4]) showed a more rapid return to zero than steady-state transpiration, but the difference was less pronounced. (c) Method comparison showing a survey measurement on sunflower. The inset graph shows full-range data with the spike in assimilation values due to opening the leaf cuvette. Dynamic assimilation stabilized faster than steady-state assimilation. (d) Leaf transpiration results from the same experiment shown in Figure 6c. Transpiration results show that the dynamic calculation approached stability faster than the steady-state calculation, but the difference was less pronounced than with CO_2 assimilation. (e) Comparison of stomatal conductance to water vapour based on dynamic or steady-state calculations [Colour figure can be viewed at wileyonlinelibrary.com]

curves with varying numbers of observations. The default parameter settings and curve-fitting method for the 'fitaci' function were used in all cases since these choices were not expected to affect the conclusions or relative comparisons presented in this work. The differences in observation number among different CO_2 response curves were not trivial: the steady-state curves contained fewer observations

($N = 17$ or less) while the dynamic assimilation curves were comprised of substantially higher numbers ($N = 550$–1,900) depending upon the CO_2 ramping rate. The effect of the additional data were clearly shown in the parameter uncertainty and the width of the 95% confidence intervals in Table 2, where the dynamic assimilation and RACiR confidence interval widths, depending upon the curve, were generally reduced by about 70%–90% relative to the steady-state confidence intervals. Overall, the reduced parameter uncertainty from dynamic assimilation should be useful for better quantifying differences among genotypes or treatments on the basis of CO_2 response curves.

Other useful applications for dynamic assimilation appeared possible, such as dynamic assimilation-based light response curves, which would reduce parameter uncertainty similar to that described above for CO_2 response curves. However, for light response curves, the differences between dynamic assimilation and steady-state measurements were less pronounced largely because CO_2 conditions inside the chamber remained near steady-state, and the correction provided by the derivative was small. The main advantage of dynamic assimilation for light response curves was in the increased total number of measurements comprising the response curve rather than increased speed when compared to steady-state measurements. In turn, the higher number of measurements will result in model fits with reduced parameter uncertainty. Good agreement between dynamic assimilation and steady-state methods was observed in cases where the ramped actinic light flux changed at a rate of about 0.8–1 μmol m^{-2} s^{-1}/s. Faster actinic ramping rates, up to about 3.3 μmol m^{-2} s^{-1}/s were attempted (data not shown) but tended to result in poor estimates of the light compensation point and quantum yield. This was possibly due to the fact that CO_2 assimilation does not instantaneously adjust to a change in actinic light levels (see Figure S2). This result also suggested that dynamic assimilation may be used in determining appropriate actinic ramping rates. For determining quantum yield, a steady-state experiment was conducted where the actinic light was changed from 120 to 0 μmol m^{-2} s^{-1} using several discrete steps over a period of 20 min, allowing 2 min per light level for assimilation to reach steady-state conditions. These were compared with a dynamic assimilation experiment which used an actinic ramping rate of 0.1 μmol m^{-2} s^{-1}/s. Thus, when the actinic intensity profile over time is identical for steady-state and DAT experiments, similar results were obtained. Increasing the actinic ramping rate over this limited range to determine quantum yield more rapidly may have been possible but was not explored.

Another application that may see benefits from dynamic assimilation are survey measurements. In both empty chamber and leaf-based experiments, the dynamic assimilation method showed stabilization in assimilation before the steady-state method. Such a result is not necessarily surprising since dynamic assimilation uses information contained in the derivative to calculate an assimilation rate even when leaf cuvette conditions are changing while the steady-state technique requires waiting for cuvette conditions to stabilize. In essence, dynamic assimilation allows for the calculation of assimilation values more quickly after the leaf cuvette closes and before the cuvette washout is complete. With optimized settings, reliable assimilation measurements could be obtained in 10–20 s, which was noticeably faster than the time required for steady-state measurement. Data from survey measurements further revealed that transpiration calculated on a dynamic basis also showed more rapid response characteristics when compared to steady-state calculations. However, water vapour typically requires a little more time to reach stability than CO_2, which is seen in the transpiration and g_{sw} data shown in Figure 7d,e. There are several likely reasons behind this behavior. For one, water is a polar molecule and adsorbs to a variety of surfaces, which results in a longer equilibration period when compared to a gas such as CO_2. Also, CO_2 assimilation and H_2O transpiration are fundamentally different processes with different behaviors in the sense that net CO_2 assimilation is driven by plant biochemistry (plant respiration and the Calvin-Benson-Bassham cycle) while transpiration is mainly driven by water potential differences caused by water exiting the stomata. Finally, stomates open and close in response to a variety of signals which impact transpiration and subsequently calculated conductance values. The observed trends in transpiration and g_{sw} calculated on a dynamic basis may have been caused by any or a combination of the above factors. This issue, though, mainly affects survey measurements since this is a condition where water vapour is not at steady-state during a significant part of the measurement window; CO_2 and light response curves are not impacted since water vapour is generally at or near steady-state conditions during the measurement.

Dynamic assimilation may prove to be useful for the determination of Γ_*, the CO_2 compensation point in the absence of day respiration (R_d) (von Caemmerer, 2000). Experiments to determine these values rely on conducting multiple CO_2 response curves on the same leaf at different sub-saturating irradiance levels (Brooks & Farquhar, 1985). The C_i at the common intersection point of the response curves is taken to be an estimate of C_*, which is the intercellular CO_2 concentration where $A = -R_d$. From a gas-exchange perspective, measurements to determine C_* can be challenging to accurately make. For one, the relevant portion of the CO_2 response curve that is needed for analysis is at low cuvette CO_2 mole fractions, which results in an inwardly directed CO_2 diffusion gradient whereby the CO_2 concentration outside the leaf cuvette is higher than CO_2 the concentration inside, which can bias measurements. Secondly, CO_2 flux into the leaf is naturally low at these mole fractions, meaning system noise as a percentage of the total flux measurement can be more problematic. Finally, each CO_2 response curve may consist of only 3–6 discrete data points, which, when coupled with the previously noted concerns, can result in regressions with high parameter (slope and intercept) uncertainty. Modern instrumentation design (high diffusion resistance, low IRGA, and control system noise) can help address the first two concerns, and the dynamic assimilation method may be useful in addressing the latter concern by providing substantially more data for CO_2 curve fitting and thereby reducing overall parameter uncertainty. In turn, this may translate to less uncertainty in C_* when averaging several intersection points or when using techniques such as the slope-intercept regression method (Walker & Ort, 2015). However, work remains to establish the suitability of dynamic assimilation for this purpose.

5 | CONCLUSIONS

The DAT represents an advancement in gas exchange techniques and a departure from the traditional steady-state paradigm. Similar to steady-state measurements, it is based on a mass balance of the leaf cuvette but does not require static conditions to make accurate CO_2 assimilation measurements. Thus, like RACiR, it enables more rapid and data-dense CO_2 response curves, but it has broader applicability and shows potential benefits for other types of measurements such as survey measurements. Dynamic assimilation shows promise in reducing uncertainty in parameter estimates and increased measurement throughput, helping to make gas exchange measurements more useful for screening and other high-throughput applications.

CONFLICT OF INTEREST

Aaron J. Saathoff has a patent submitted on rapid response curves and the dynamic mass balance. Aaron J. Saathoff and Jon Welles have a patent submitted on the rangematch feature in the LI-6800.

DATA AVAILABILITY STATEMENT

The data that supports the findings of this study are available in the supplementary material of this article.

ORCID

Aaron J. Saathoff https://orcid.org/0000-0001-8715-9978

REFERENCES

Ainsworth, E. A., Serbin, S. P., Skoneczka, J. A., & Townsend, P. A. (2014). Using leaf optical properties to detect ozone effects on foliar biochemistry. *Photosynthesis Research*, *119*(1), 65–76.

Bloom, A. J., Mooney, H. A., Björkman, O., & Berry, J. (1980). Materials and methods for carbon dioxide and water exchange analysis. *Plant, Cell & Environment*, *3*(5), 371–376.

Brooks, A., & Farquhar, G. D. (1985). Effect of temperature on the CO_2/O_2 specificity of ribulose-1,5-bisphosphate carboxylase/oxygenase and the rate of respiration in the light. *Planta*, *165*(3), 397–406.

Coursolle, C., Otis Prud'homme, G., Lamothe, M., & Isabel, N. (2019). Measuring rapid A–ci curves in boreal conifers: Black spruce and balsam fir. *Frontiers in Plant Science*, *10*, 1276.

Duursma, R. A. (2015). Plantecophys - an R package for analysing and modelling leaf gas exchange data. *PLoS One*, *10*(11), e0143346.

Eaton, J. W., Bateman, D. & Hauberg, S. (2018). GNU Octave version 4.4.1 manual: A high-level interactive language for numerical computations. Retrieved from https://www.gnu.org/software/octave/doc/v4.4.1/

Ehrlich, P. R., & Harte, J. (2015). Opinion: To feed the world in 2050 will require a global revolution. *Proceedings of the National Academy of Sciences*, *112*(48), 14743–14744.

Farquhar, G. D., von Caemmerer, S., & Berry, J. A. (1980). A biochemical model of photosynthetic CO_2 assimilation in leaves of C_3 species. *Planta*, *149*(1), 78–90.

Fu, P., Meacham-Hensold, K., Guan, K., & Bernacchi, C. J. (2019). Hyperspectral leaf reflectance as proxy for photosynthetic capacities: An ensemble approach based on multiple machine learning algorithms. *Frontiers in Plant Science*, *10*, 730.

Gu, L., Pallardy, S. G., Kevin, T., Law, B. E., & Wullschleger, S. D. (2010). Reliable estimation of biochemical parameters from C_3 leaf photosynthesis–intercellular carbon dioxide response curves. *Plant, Cell & Environment*, *33*(11), 1852–1874.

Heinicke, A. J., & Hoffman, M. B. (1933). An apparatus for determining the absorption of carbon dioxide by leaves under natural conditions. *Science*, *77*(1985), 55–58.

Jaggard, K. W., Qi, A., & Ober, E. S. (2010). Possible changes to arable crop yields by 2050. *Philosophical Transactions of the Royal Society, B: Biological Sciences*, *365*(1554), 2835–2851.

Laisk, A. & Oja, V. (1998). Dynamics of leaf photosynthesis: Rapid response measurements and their interpretations: CSIRO. https://ebooks.publish.csiro.au/content/dynamics-leaf-photosynthesis#tab-info

Laisk, A., & Walker, D. A. (1986). Control of phosphate turnover as a rate-limiting factor and possible cause of oscillations in photosynthesis: A mathematical model. *Proceedings of the Royal Society of London, Series B: Biological Sciences*, *227*(1248), 281–302.

Lawrence, E. H., Stinziano, J. R., & Hanson, D. T. (2019). Using the rapid A-C_i response (RACiR) in the li-Cor 6400 to measure developmental gradients of photosynthetic capacity in poplar. *Plant, Cell & Environment*, *42*(2), 740–750.

Long, S. P., & Bernacchi, C. J. (2003). Gas exchange measurements, what can they tell us about the underlying limitations to photosynthesis? Procedures and sources of error. *Journal of Experimental Botany*, *54*(392), 2393–2401.

Long, S. P., Farage, P. K., & Garcia, R. L. (1996). Measurement of leaf and canopy photosynthetic CO_2 exchange in the field. *Journal of Experimental Botany*, *47*(11), 1629–1642.

Long, S. P., & Hällgren, J.-E. (1993). Measurement of CO_2 assimilation by plants in the field and the laboratory. In D. O. Hall, J. M. O. Scurlock, H. R. Bolhar-Nordenkampf, R. C. Leegood, & S. P. Long (Eds.), *Photosynthesis and production in a changing environment* (pp. 129–167). New York, NY: Chapman & Hall.

Long, S. P., & Ireland, C. R. (1985). The measurement and control of air and gas flow rates for the determination of gaseous exchanges of living organisms. In B. Marshall & F. I. Woodward (Eds.), *Instrumentation for environmental physiology* (pp. 123–137). Cambridge, England: Cambridge University Press.

McLean, F. T. (1920). Field studies of the carbon dioxide absorption of coco-nut leaves. *Annals of Botany*, *34*(3), 367–389.

Miao, Z., Xu, M., Lathrop, R. G., Jr., & Yufei, W. (2009). Comparison of the A–C_c curve fitting methods in determining maximum ribulose 1·5-bisphosphate carboxylase/oxygenase carboxylation rate, potential light saturated electron transport rate and leaf dark respiration. *Plant, Cell & Environment*, *32*(2), 109–122.

Mooney, H. A. (1972). Carbon dioxide exchange of plants in natural environments. *Botanical Review*, *38*(3), 455–469.

Mooney, H. A., Dunn, E. L., Harrison, A. T., Morrow, P. A., Bartholomew, B., & Hays, R. L. (1971). A mobile laboratory for gas exchange measurements. *Photosynthetica*, *5*(2), 128–132.

Perdomo, J. A., Sales, C. R. G., & Carmo-Silva, E. (2018). Quantification of photosynthetic enzymes in leaf extracts by immunoblotting. In S. Covshoff (Ed.), *Photosynthesis methods and protocols* (pp. 215–227). Totowa, NJ: Humana Press.

Pilon, C., Snider, J. L., Sobolev, V., Chastain, D. R., Sorensen, R. B., Meeks, C. D., … Earl, H. J. (2018). Assessing stomatal and non-stomatal limitations to carbon assimilation under progressive drought in peanut (*Arachis hypogaea* L.). *Journal of Plant Physiology*, *231*, 124–134.

R Core Team (2019). R: A language and environment for statistical computing. Retrieved from https://www.R-project.org/

Ray, D. K., Mueller, N. D., West, P. C., & Foley, J. A. (2013). Yield trends are insufficient to double global crop production by 2050. *PLoS One*, *8*(6), e66428.

Sharkey, T. D. (2016). What gas exchange data can tell us about photosynthesis. *Plant, Cell & Environment*, *39*(6), 1161–1163.

Sharkey, T. D. (2019). Is triose phosphate utilization important for understanding photosynthesis? *Journal of Experimental Botany*, *70*(20), 5521–5525.

Sharkey, T. D., Bernacchi, C. J., Farquhar, G. D., & Singsaas, E. L. (2007). Fitting photosynthetic carbon dioxide response curves for C_3 leaves. *Plant, Cell & Environment*, *30*(9), 1035–1040.

Sharkey, T. D., Stitt, M., Heineke, D., Gerhardt, R., Raschke, K., & Heldt, H. W. (1986). Limitation of photosynthesis by carbon metabolism. II. O_2-insensitive CO_2 uptake results from limitation of triose phosphate utilization. *Plant Physiology*, *81*(4), 1123–1129.

Silva-Perez, V., Molero, G., Serbin, S. P., Condon, A. G., Reynolds, M. P., Furbank, R. T., & Evans, J. R. (2017). Hyperspectral reflectance as a tool to measure biochemical and physiological traits in wheat. *Journal of Experimental Botany*, *69*(3), 483–496.

Spoehr, H. A., & McGee, J. M. (1924). Investigations in photosynthesis. *Industrial and Engineering Chemistry*, *16*(2), 128–130.

Stinziano, J. R., Adamson, R. K., & Hanson, D. T. (2019). Using multirate rapid a/C_i curves as a tool to explore new questions in the photosynthetic physiology of plants. *New Phytologist*, *222*(2), 785–792.

Stinziano, J. R., McDermitt, D. K., Lynch, D. J., Saathoff, A. J., Morgan, P. B., & Hanson, D. T. (2019). The rapid a/C_i response: A guide to best practices. *New Phytologist*, *221*(2), 625–627.

Stinziano, J. R., Morgan, P. B., Lynch, D. J., Saathoff, A. J., McDermitt, D. K., & Hanson, D. T. (2017). The rapid A–C_i response: Photosynthesis in the phenomic era. *Plant, Cell & Environment*, *40*(8), 1256–1262.

Strain, B. R. (1969). Seasonal adaptations in photosynthesis and respiration in four desert shrubs growing *in situ*. *Ecology*, *50*(3), 511–513.

Taylor, S. H., & Long, S. P. (2019). Phenotyping photosynthesis on the limit – A critical examination of RACiR. *New Phytologist*, *221*(2), 621–624.

Tester, M., & Langridge, P. (2010). Breeding technologies to increase crop production in a changing world. *Science*, *327*(5967), 818–822.

Thomas, M. D., & Hill, G. R. (1937). The continuous measurement of photosynthesis, respiration, and transpiration of alfalfa and wheat growing under field conditions. *Plant Physiology*, *12*(2), 285–307.

von Caemmerer, S. (2000). *Biochemical models of leaf photosynthesis*. Collingwood, Australia: CSIRO Publishing.

Walker, B. J., & Ort, D. R. (2015). Improved method for measuring the apparent CO_2 photocompensation point resolves the impact of multiple internal conductances to CO_2 to net gas exchange. *Plant, Cell & Environment*, *38*(11), 2462–2474.

Wang, Q., Chun, J. A., Fleisher, D., Reddy, V., Timlin, D., & Resop, J. (2017). Parameter estimation of the Farquhar—von Caemmerer—Berry biochemical model from photosynthetic carbon dioxide response curves. *Sustainability*, *9*(7), 1288.

SUPPORTING INFORMATION

Additional supporting information may be found in the online version of the article at the publisher's website.

How to cite this article: Saathoff, A. J., & Welles, J. (2021). Gas exchange measurements in the unsteady state. *Plant, Cell & Environment*, *44*(11), 3509–3523. https://doi.org/10.1111/pce.14178